Tethys, 4, 11–18, 2007
www.tethys.cat
ISSN-1697-1523
eISSN-1139-3394
DOI:10.3369/tethys.2007.4.02

Journal edited by **ACAM**
(Associació Catalana de Meteorologia)

Effects of solar height, cloudiness and temperature on silicon pyranometer measurements.

A. Raïch, J. A. González and J. Calbó

Grup de Física Ambiental, Departament de Física i Institut de Medi Ambient, Universitat de Girona, Campus Montilivi, EPS-II, 17071 Girona

Received: 24-I-2007 – Accepted: 20-VII-2007 – **Translated version**

Correspondence to: jose.gonzalez@udg.es

Abstract

The objective of the paper is to improve the agreement between the global irradiance measurements taken with a Kipp & Zonen CM11 thermoelectric pyranometer, and several Li-Cor Li200SA photovoltaic (silicon) pyranometers. With this purpose, we propose some corrections for the angular response of the sensors, which in general moves away from the ideal cosine response. The 1-minute data corresponding to an annual cycle of irradiance measurements taken by both types of pyranometers in the radiometric station of the University of Girona have been analysed. Corrections suggested by the angular response of instruments are based on previous studies, as well as simulations made using a multi-layer and spectral radiative transfer model. The simulation allowed us to obtain corrections to compensate for the different angular and spectral responses of both types of instruments. For clear skies, angular and spectral corrections significantly improve the agreement between the measurements of both types of pyranometers. An empirically obtained correction of the effect of temperature on the measurement of silicon pyranometers is also suggested. Despite the fact that corrections have been obtained for clear skies, they have also been applied to cloudy sky conditions, objectively characterised through an algorithm based on global and diffuse irradiance measurements. Finally, it is verified that the corrections also improve the agreement between measurements of the two types of sensors independently from the cloud cover extension.

1 Introduction

Short wave solar radiation (from 280 to 4000 nm) represents the most important source of energy of our planet. This energy reaches the atmosphere, hydrosphere and biosphere, producing a series of phenomenon which affect it. The behaviour of climatic and ecological systems are impelled and modulated at all scales, from the most local to the most global, by the entrance of energy linked to radiation.

Consequently, precise knowledge of short wave solar radiative levels, at any point of the atmosphere-ocean-surface system, is vital. Validation of radiative transfer models in the atmosphere (both the most rigorous as well as the parameterised ones or those that form part of climate models) with experimental measurements requires extensive and accurate information.

Therefore, in an initially discoordinate way between the different countries, a global network of radiation sensors which are preferentially devoted to the quantification of this energetic resource has begun to grow. An example of this is the fact that in Catalonia, since the 1980's, there has been a radiometric network belonging to the Institut Català d'Energia, which periodically updates the Solar Atlas of Catalonia (ICAEN, 2001). The increasing interest in improving the knowledge of the role of radiation in natural systems has also led to the development of large projects for its measurement both from surface stations and from satellite instruments or, although more seldomly, from planes, ships and other means.

One of the most well known examples of these efforts is the ARM project (Atmospheric Radiation Measurement; Ackerman and Stokes, 2003) dedicated to the careful measurement of radiative levels on terrestrial surface, which is crucial for determining the validity and precision of radiative transfer models applied to different real atmospheric situa-

tions: clouds, turbidity, water vapour, etc. A further example is the BSRN network (Baseline Surface Radiation Network, propuesta por el World Climate Research Program; Ohmura et al., 1998) put forward by the World Climate Research Program to perform precise measurements on surface, to be used for the validation of satellite measurements and radiative codes in climate models, and the monitoring of potential long-term changes in irradiance (Perez et al., 2001).

In the last few years, the creation of a good radiative database has been a global and prioritised aim, while efforts have been made to coordinate different measurement networks. Furthermore, since solar radiation is a phenomenon with a high spatial and temporal variability, the sensor network has to be as extensive as possible, mainly in order to cover those regions that represent higher geographical and climatic diversity. The cost of high-quality sensors and of the maintenance of stations has historically been a limitation for the achievement of a bigger network extension.

In a practical sense, the most relevant radiometric magnitude in the quantification of solar radiation is global irradiance on a horizontal surface (E_g). This is considered, for the terrestrial surface, as the composition of two irradiances: direct irradiance (E_b) which comes directly from the solar disc, and diffuse irradiance (E_d), which comes from all other directions of the sky. Both irradiances relate to one another according to the expression:

$$E_g = E_b \cos(SZA) + E_d \tag{1}$$

where SZA is the solar zenith angle.

The BSRN considers that the best measurement of global horizontal irradiance is obtained through the sum of the direct component, measured using a cavity radiometer, and the diffuse component, measured by a first class pyranometer with a shadowing disc. With this method, the repeatability of the measurement is around 10 W m^{-2}, better than that obtained when measuring global irradiance with only one pyranometer (Perez et al., 2001). However, in radiometric stations, the use of pyranometers for global irradiance measurement is common due to the inherent difficulties of the first method, such as the cost of instruments, calibrations, and the need for a solar tracking system. Among other characteristics, the ideal pyranometer would present an angular response correctly reproducing the effect of the projection of the beam on a horizontal surface (cosine response). As real instruments only approach this response, they should be characterised carefully in order to obtain good measurements.

Nowadays, the most commonly used pyranometers are thermopile type sensors and solar cells. The first take advantage of thermoelectric effect to generate tensions according to the temperature difference between two surfaces with different absorption capacities of radiation. Examples of thermoelectric pyranometers are the Eppley PSP and the Kipp & Zonen CM11, which are classified as first class according to the criteria of the World Meteorological Organisation. In the second case, solar cells, the photovoltaic effect is used in semiconductors (usually silicon) to obtain a current which is much strongerwho also suggested the incorporation of an acrylic diffuser with a convenient profile to improve the angular response. The main disadvantages of these instruments, however, are its spectral response (which is much less uniform and more limited than that of thermoelectric instruments), the dependence of the response on temperature, and the initial ageing, which is reflected in a gradual change of the instrument sensitivity when the radiation is more intense. These silicon sensor pyranometers are largely used in meteorological stations due to their lower cost, and in fact, one of the product's manufacturers, Li-Cor, produced more than 31000 units in 1997 (King et al., 1998). The use of solar cells as pyranometers was put forward by Kerr et al. (1967), who also suggested the incorporation of an acrylic diffuser with a convenient profile to improve the angular response. The main disadvantages of these instruments, however, are its spectral response (which is much less uniform and more limited than that of thermoelectric instruments), the dependence of the response on temperature, and the initial ageing, which is reflected in a gradual change of the instrument sensitivity.

Regarding the first limitation of these instruments, it must be stated that the radiation spectrum depends basically on atmospheric conditions, solar height and optical properties (particularly albedo) of surfaces surrounding the measurement location. The spectral structure of global irradiance does not experience as significant changes in the visible band (i.e. between conditions of clear skies and cloudy skies) as those which occur in the infrared band. However, the same manufacturer of silicon pyranometers Li-Cor, based on the Federer and Tanner (1965) and Kerr et al. (1967), studies, admits that the response in cloudy conditions may be 10% higher than the response for clear skies due to the differences between the radiation spectrums of both cases.

Here we present the main results of a study (Raïch, 2006) which intends to compare solar global irradiance measurements taken with photovoltaic or silicon sensors with thermoelectric pyranometer measurements, which have been taken as reference. Corrections reducing the effect of differences between angular and spectral responses of the instruments have been suggested and applied. Finally, we have studied the effects of temperature and cloudiness on the ratio between both measurements already corrected:

$$r = \frac{E_g^{PV}}{E_g^{TP}} \tag{2}$$

where E_g^{PV} and E_g^{TP} represent global irradiances measured by photovoltaic and thermoelectric pyranometers respectively, and r its quotient or ratio.

2 Methodology

2.1 Preparation of the database

For this study we have used two Kipp & Zonen CM11 thermoelectric pyranometers (one for the measurement of global irradiance and the other with a shadow band for the measurement of diffuse irradiance), and three Li-Cor Li200SA photovoltaic pyranometers, two of which were equipped with thermocouples for the monitoring of the sensors temperature. All these instruments are located on the terrace of the PII building of the Escola Politècnica Superior of the University of Girona (41° 58'18.19" N, 2° 49' 3.57" E, 100 m a.s.l). Automated measurements are taken every second by means of data acquisition devices (datalogger Cambpell CR10). Inside the datalogger box there is the shunt element (with a temperature rate measured in the laboratory lower than $1.4{\cdot}10^{-5}$ °C^{-1} por debajo de los 50°C) which transforms the intensities provided by the photovoltaic pyranometers in measurable voltages. Measurements are averaged or integrated at different intervals (in the case of irradiance and temperature, every minute), and they are periodically downloaded by a computer system, in which a database is built. Some data is presented in real time on the internet (http://copernic.udg.es/cat/meteorologica.php).

The studied database starts in the year 2000 (when the recordings taken every minute began) and finishes in July 2001 (when the two photovoltaic pyranometers incorporating temperature sensors were removed from the station). The measurements included in the database correspond to several global irradiance registers (one of them obtained from a CM11 and the other three from Li200SA sensors), diffuse irradiance, and their respective standard deviations within the recording interval. Diffuse irradiance was measured with a CM11 with a shadow band of the Eppley type which was adjusted from 1 to 3 times a week. Uncertainty associated with diffuse irradiance measured in this way is approximately 5% (Drummond, 1964). Other variables included in the database are the temperatures of the two photovoltaic sensors and the inner temperature of the box where the dataloggers are installed (all these temperatures were measured with an accuracy of $\pm$ 0.1°C); in addition, temperature and environmental relative humidity are also included, among other meteorological data.

In terms of data processing, the first step was to correct diffuse irradiance measurements using a correction method for the part of the sky screened by the shadow band. The method proposed by LeBaron et al. (1990), was chosen to perform a correction accounting for the geometry of the shadow band, the solar height and the sky conditions.

The difficulty in establishing objective criteria for choosing the periods of clear sky from a visual inspection of irradiance graphs depending on time is well known. Furthermore, the extension of the study for cloudy skies was significantly restricted due to the absence of a complete register of cloud fraction (cf) either from visual observations or from a hemispherical photographic camera that was later installed in the station (Long et al., 2006). To resolve this limitation, the method suggested by Long and Ackerman (2000), which will from now on be referred to as the LA method, was applied to the database. With this method, from the 1-minute global and diffuse irradiance measurements and the application of a series of 4 tests, we obtained 15-minute averaged values of global and diffuse irradiance and the rest of the variables included in the files, and, more importantly, an estimation of cloud fraction. The method is limited, however, to periods with $SZA \leq 80°$.

The zenith angle value used in every register of 15 minutes is the central value of the period, calculated using the formula described in Icqbal (1983). It is also the value used in all the subsequent corrections. The SZA value obtained when applying the LA method (by averaging of the cosine of SZA of the 1-minute data within the interval) is not precise enough in either certain periods of the day or certain seasons of the year in which SZA changes fast.

Finally, the daily files were compiled into an annual file and a final filter was applied to eliminate some clearly abnormal ratio values. These abnormal values mostly corresponded to exceptionally low measurements of some of the pyranometers (circumstances produced by occasional shadowing caused by the maintenance of the station or by the presence of birds). This filtering affected only 0.4% of all the values analysed.

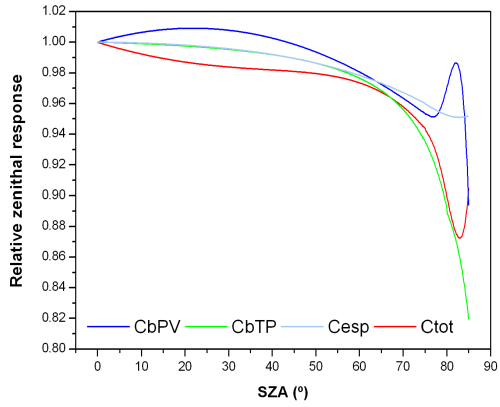

Figure 1. Responses, relative to normal incidence, of CM11 and Li200SA pyranometers (*CbTP*, in green and *CbPV*, in navy blue), from Michalsky et al. (1995) data. In light blue, spectral correction by Li200SA, relative to CM11 spectral correction, obtained from simulations with a radiative transfer model. In red, total correction ($Ctot$), which is applied to the ratio between Li200SA and CM11 measurements. SZA is the solar zenith angle.

2.2 The obtaining of angular and spectral corrections

Differences between instruments, which we wish to correct, come from their angular response (cosine response) and from their spectral response (different sensitivities in each wavelength of the received radiation). Firstly, angular corrections for each of the pyranometers are approached.

Thus, we firstly considered the response of instruments in two ideal conditions: supposing that they only received direct radiation or only diffuse radiation. It was possible to determine correction factors to be applied in each case from information published by Michalsky et al. (1995). Specifically, in the case of the CM11 thermoelectric instrument and the Li200SA photovoltaic instrument subjected to pure direct radiation, analytical expressions respectively describing their response depending on zenith angle (*CbTP* and *CbPV*) were extracted from the diagrams shown in Figure 1. For the same instruments, but subjected to pure isotropic diffuse irradiance, the correction factor to be applied is constant (*CdTP* = 0.9789 and *CdPV* = 0.9900 respectively).

In addition, measurements carried out by pyranometers were numerically simulated so that they were comparable against each other, using a spectral and multilayer radiative transfer model, specifically SBDART (Santa Barbara DISORT Atmospheric Radiative Transfer) version 1.5 developed by Ricchiazzi et al. (1998), which resolves the equation of radiative transfer numerically integrating it with the DISORT algorithm, and considering each atmospheric layer horizontally homogeneous. Some of the input variables of this model remained unchanged in all simulations: atmospheric model (US62 atmosphere has been used), height (0 m), relative humidity (50%), aerosol (rural), cloud profile (clear sky), filter functions to simulate spectral responses of instruments (we have introduced one which corresponds to the Li200SA response, whereas no filter was applied for the CM11), wavelengths (for the CM11 from 300 nm to 2800 nm and for the Li200SA from 400 nm to 1100 nm, both with increments of 4 nm). Other conditions were changed: albedo (from 0 to 0.30, in increments of 0.05), ozone column (from 0.25 to 0.45 atmcm, in increments of 0.05 atm-cm), precipitable water column (from 0.5 to 4 cm, in increments of 0.5 cm), aerosol opacities at 550 nm (from 0 to 0.6, in increments of 0.1) and the zenith angle (from 0 to 85°, in increments of 5°).

To obtain overall corrections for the two pyranometers, we have to combine both previous factors. It is for this reason that Hay-Davies diffuse radiation redistribution was considered, see Duffie and Beckman (1991), that is to say, the circumsolar part of the diffuse radiation receives the same angular correction as the direct part, whereas the rest is treated as an isotropic contribution. The circumsolar component of the diffuse is that part scattered in directions very close to solar beam, and therefore it presents an incidence angle on sensors very close to that of the direct component.

Then, the corrections for global irradiances are calculated, always based on simulations, in the following manner:

$$\begin{aligned} E^{PV}_{global,corrected} &= (E^{PV}_{direct} + A_i \cdot E^{PV}_{diffuse})\, CbPV + \\ &\quad (1 - A_i)\, E^{PV}_{diffuse} \cdot CdPV \\ E^{TP}_{global,corrected} &= (E^{TP}_{direct} + A_i \cdot E^{TP}_{diffuse})\, CbTP + \\ &\quad (1 - A_i)\, E^{TP}_{diffuse} \cdot CdTP \end{aligned} \tag{3}$$

where A_i is the index of anisotropy defined by Hay-Davies, $A_i = \frac{E^{TP}_{direct}}{E_{sc}\ \cos(SZA)}$ and $E^{PV,TP}_{dir,dif}$ is the simulated values of direct and diffuse irradiance. Solar constant, E_{sc} takes the 1367 W m^{-2} value. Finally, the coefficients of angular correction of global irradiances of both instruments (*CgTP* and *CgPV* respectively) are obtained dividing simulated global irradiance values by the corrected values obtained in expression (3). These are the coefficients used to correct the real measurements of global irradiance.

Once the angular responses of instruments have been corrected, we have to consider their different spectral response. Considering CM11 as a reference and using the previous simulations with SBDART, the factor of spectral correction, $Cesp$, which has to be applied to the Li200SA measurements so that they reproduce those of CM11 (see Fig. 1) is determined. This factor will depend on SZA. Combining the presented corrections we can find the total correction ($Ctot = \frac{CgTP \cdot Cesp}{CgPV}$), so that dividing the r ratio (see Eq. 2) by $Ctot$, we will obtain the ratio corrected for the different cosine and spectral responses. This total correction is also presented in Figure 1, where the dependence on the zenith angle is demonstrated. When applied, the ratio would have to produce a value of 1, if all pyranometers were correctly calibrated, and supposing there were no variations due to other factors which could affect the ratio (such as the temperature of sensors and cloudiness).

3 Results

We now present the results of applying the total correction ($Ctot$) to the database, for later ascertaining the effects of temperature and cloudiness on the ratio between the measurements of both types of pyranometers.

3.1 Analysis for clear skies

To obtain the cases corresponding to clear skies from the Girona 2000-2001 database (formed by 13792 records of 15 min obtained through the application of the LA algorithm to the 1-minute data), a threshold of $cf \leq 0.02$ has been established on the cloud fraction. Thus, we have obtained a subgroup of 2659 registers, to which $Ctot$ has been applied to the ratio of global irradiances of both instruments.

The impact of this angular and spectral correction ($Ctot$) on original data can be observed in Figure 2, where

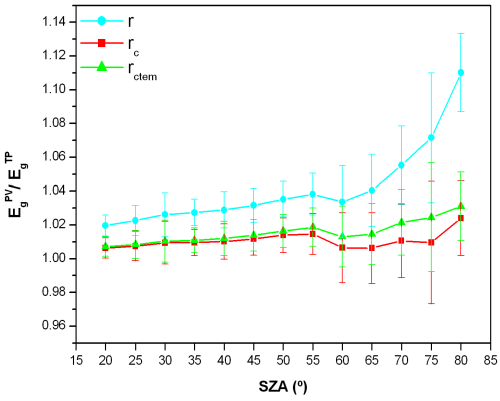

Figure 2. Effect of angular and spectral corrections (red) and temperature correction (green) on original ratios for clear sky conditions (light blue). Bars represent the standard deviations inside each SZA interval. Only results for pyranometer 3 are shown.

Table 1. Standard deviation of the ratios for clear sky registers (r_c is the ratio angularly and spectrally corrected, r_{ctem} incorporates temperature correction).

Li200SA	r	r_c	r_{ctem}
1	0.034	0.029	0.028
2	0.023	0.020	0.019
3	0.022	0.018	0.016

it is shown that from 60° its contribution is significant. In Fig. 2, the results for a unique photovoltaic pyranometer are presented, however the result of applying the corrections is similar in the other two cases. Quantitatively, by means of standard deviation (SD) of the ratios, we can assess the decrease in this index in Table 1, after applying the correction, which is approximately 17% (average for the three photovoltaic pyranometers), even if, as it can be observed in Fig. 2, the relative improvement is more remarkable for large zenith angles.

In Figure 3, we can observe the dependence of the ratio (after having applied the $Ctot$ angular and spectral correction to clear skies data) upon the measured temperature in the Li200SA themselves. We can attribute this dependence to silicon pyranometers, as the CM11 measurement has been considered as reference due to its effective mechanism of temperature compensation, disagreements <1% between -10 y +40°C, Manual CM11 Kipp and Zonen (2006). For the three silicon pyranometers we can observe a non-linear dependence on temperature and that the temperature coefficient strongly depends on the chosen temperature interval. Thus, for temperatures less than 20°C, the ratio presents strong increases of up to $3.0{\cdot}10^{-3}$ °C^{-1}; from 20 to 30°C, increases are more and more moderate; and for temperatures higher than 35°C a saturation is reached. The Manual Li-Cor (2006) specifies a maximum temperature coefficient for the Li200SA of $1.5{\cdot}10^{-3}$ °C^{-1}, whereas for our database, if we average coefficients between 10°C i 45°C, we obtain a temperature coefficient of $1.3{\cdot}10^{-3}$ °C^{-1}, which is in strong accordance with specifications if we assume a linear dependence. King et al. (1998) give a value of $0.82{\cdot}10^{-3}$ °C^{-1} for the Li200SA coefficient and Michalsky et al. (1987) of $0.6{\cdot}10^{-3}$ °C^{-1}, always from measurements carried out in laboratories. These disagreements are not unusual considering the behaviour of the Li200SA with temperature: linear increase for low temperatures and stabilisation above 30°C. We must also point out that this behaviour has been confirmed with daily evolutions of the ratio and in other annual cycles.

To obtain an empirical correction of Li200SA sensor temperature effects, the values of angularly and spectrally corrected ratios presented in Figure 3 are normalised, dividing them by the value corresponding to the 35°C interval (in which temperature already has a negligible effect). This normalised ratio is then adjusted to a function of the type: $1 - e^{\frac{-(t-t_0)}{t_1}}$, where t is sensor temperature, and t_0 and t_1 two parameters. A function of this kind appropriately describes the aforementioned behaviour of the ratio depending on temperature. The adjusted function is also presented in Figure 3, and the effect of the application of this temperature correction, for one of the sensors, is presented in Figure 2. After application, SD of angularly and spectrally previously corrected ratios improves additionally on an average of 7% (see Table 1).

For the most general case in which we only have at our disposal environmental temperature registers, an empirical expression has been adjusted relating the sensor temperature (t) to air temperature (t_{air}) and Li200SA measured irradiance (E_g^{PV}):

$$t = 0.99327\, t_{air} - 0.00001\, (E_g^{PV})^2 + 0.02041\, E_g^{PV} + 1.45113 \quad (4)$$

3.2 Analysis for cloudy skies

The same analysis explained in the previous section has been repeated for all data, regardless of the state of sky, that is to say, of the cloud fraction. The results for one of the pyranometers are presented in Figure 4. As expected, due to the Li200SA behaviour (higher temperature rates for lower temperatures), the effect of temperature correction is more obvious for large zenith angles (which correspond to sunrise and sunset, and to winter situations in general, when the temperature is usually lower). SD does not improve, since dispersion increase introduced by clouds exceeds by far the global improvement introduced by corrections for clear skies (which is 24% as a whole, as we said before).

Finally, to see how angular and spectral corrections

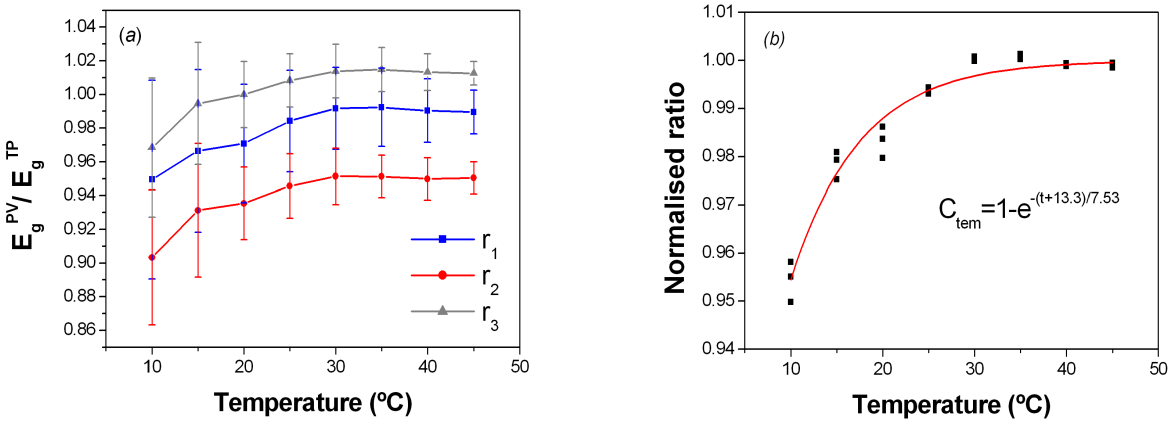

Figure 3. (a) For clear skies, dependence of Li200SA pyranometers response on the temperature (having applied the angular and spectral corrections) and respective standard deviations; (b) adjusted function from normalised ratios, $Ctem$, in which t is the temperature measured in the same sensor.

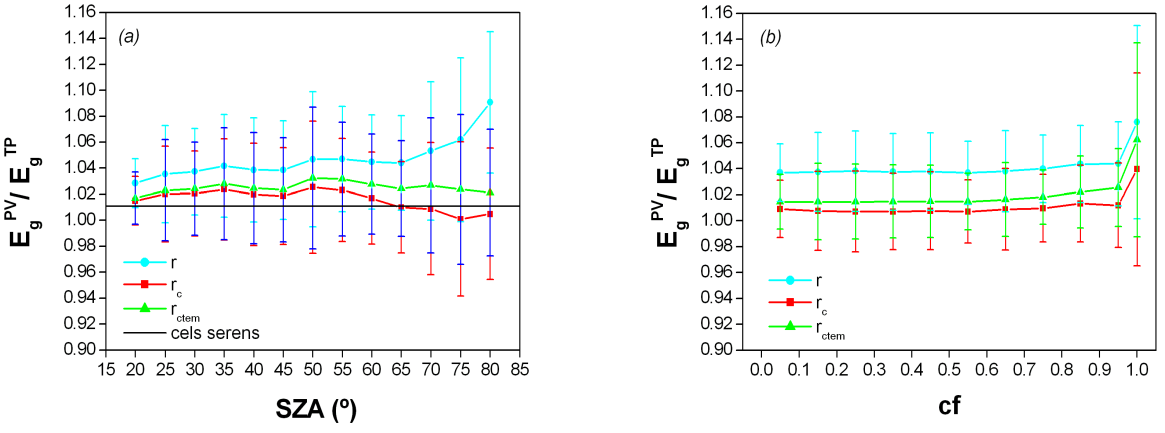

Figure 4. (a) Corrections behaviour depending on the zenith angle for all type of cloudy skies. The role of the temperature correction for large zenith angles stands out. The horizontal line represents the mean ratio for clear skies: (b) The same but depending on cloud fraction (cf). A 4% increase in ratio and the doubling of standard deviation for the cf case strictly equal to 1, that is to say, for totally covered skies, stands out. In both cases, results for pyranometer 3 are shown.

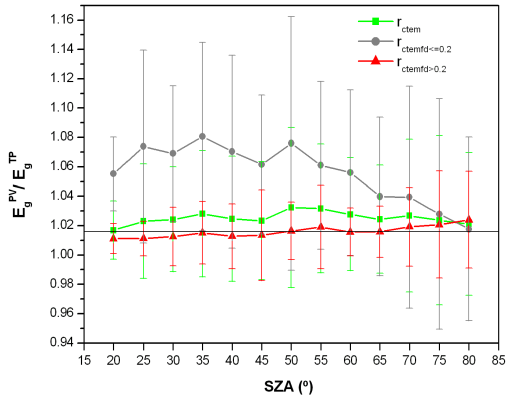

Figure 5. Corrected ratio depending on SZA. In dark grey, values for conditions with direct fraction $df \leq 0.2$ (blocked out sun); in red, values for $df > 0.2$; in green, values including all conditions. The horizontal line represents the mean ratio for clear skies. The results are shown for pyranometer 3.

behave depending on cloud fraction, a study for cf intervals (with increments of 0.1 and separating those strictly equal to 1) has been carried out. The results are also presented in Figure 4 and we can ascertain that total correction is maintained throughout the whole cf range of values, except for those strictly equal to 1 (totally overcast skies) where ratios increase by approximately 4% and the dispersion is doubled regarding the previous intervals (characteristics already present in the original data before applying any type of correction). This disagreement is ascribed to an important contribution of diffuse irradiance which has not been taken into account in the modelling (which was for clear skies) and which in these circumstances, of completely overcast skies, is much more clearly shown than for partially clouded skies.

Thus, in Figure 5, we can observe that for registers with a direct fraction less than or equal to 0.2 (a situation in which the diffuse component is almost the only existent) the Li200SA measured irradiance increases by more than 4% regarding the values measured for all type of skies data, in zenith angles inferior to 60°, and decreases for greater zenith angles. To reinforce this statement the complementary group has also been represented (data with direct fraction greater than 0.2) which on the whole behave as clear skies registers, despite including sky conditions which are largely heterogeneous (but always with visible sun, that is to say, with the presence of direct beam).

4 Conclusions

A series of expressions have been presented which correct the angular and spectral responses, as well as the temperature effect of Li200SA photovoltaic sensor regarding CM11 thermoelectric sensor, for clear skies conditions. Corrections to angular and spectral responses of both instruments are analytical functions that depend on the solar zenith angle. Their application has allowed us to uncover dependence on temperature of the Li200SA response: below 20°C there is a tendency for linear asymptotic behaviour and above 35°C this levels out. This behaviour so linked to the studied temperature interval, explains the great variability of Li200SA temperature coefficients present in scientific literature. A possible technological application to counteract the globaltemperature irradiance characteristic would be to maintain the Li200SA sensors and in general all photovoltaic sensors at a constant temperature of 35°C, mainly in climates colder than that of the Mediterranean.

The impact of both corrections (angular and spectral) and that of Li200SA temperature is a clear improvement on measurements. Specifically, the SD of the ratio decreases in 24% for clear skies situations. For cloudy skies, the angular and spectral correction behaves very well for all cloud fraction situations, except in the case of totally overcast skies, in which, even after applying the corrections, the global irradiance measured by Li200SA is 4% higher than that measured by CM11. This particular behaviour for totally overcast skies is also associated with a duplication of dispersion. The impact of temperature correction seems to be larger in cloudy skies but this increase in improvement only shows up in relative measurements and it remains masked by the dispersion increase introduced by cloudiness, mainly for situations with large zenith angles (that is why they do not appear in SD of data corresponding to all types of sky).

It would be of interest for future studies to analyze the effect of temporal integration on results, as the temporal responses of both instrument families are very different (20 s for CM11 and 10 μs for Li200SA). The present paper has been based on 15-minute periods, in which some of the radiation characteristics could be lost, especially in partially cloudy sky conditions. A justification from physical models of the Li200SA irradiance-temperature characteristic which would allow us to generalise the results to all photovoltaic pyranometers remains pending. Since daily irradiation is a relevant information in energetic applications, it should be established the way in which corrections for short time irradiances improve the agreement between daily irradiations measured with both types of sensors.

Acknowledgements. This article is an abstract of the Research Paper presented by the first author in July 06 in the framework of the Environment Doctorate Program of the University of Girona. This research has been possible thanks to the help and collaboration of both directors of this paper: Dr. Josep A. González and Dr. Josep Calbó, and it has been developed within the Environmental Physics Group of UdG in the framework of the NUCLIER, MEC CGL 2004-02325 project (http://copernic.udg.es/gfa/nuclier/nuclier.htm).

References

Ackerman, T. and Stokes, G. M., 2003: *The Atmospheric Radiation Measurement program*, Phys Today, **56**, 38–4.

Drummond, A. J., 1964: *Comments on "Sky radiation measurement and corrections"*, J Appl Meteorol, **3**, 810–811.

Duffie, J. A. and Beckman, W. A., 1991: Solar Engineering of Thermal Processes, John Wiley and Sons, Inc., New York.

Federer, C. A. and Tanner, C. B., 1965: *A simple integrating pyranometer for measuring daily solar radiation*, Journal of Geophysics, **70**, 2301–2306.

ICAEN, 2001: Atles de radiació solar de Catalunya., Edició 2000, Generalitat de Catalunya, Barcelona.

Icqbal, M., 1983: An introduction to solar radiation, Academic, New York.

Kerr, J. P., Thurtell, C. B., and Tanner, C. B., 1967: *An integrating pyranometer for climatological observer stations and mesoscale networks*, J Appl Meteorol, **6**, 688–694.

King, D. L., Boyson, W. E., and Hansen, B. R., 1998: Improved accurancy for low-cost solar irradiance sensors., Sandia National Laboratories.

Kipp and Zonen, 2006: Manual CM 11, www.kippzonen.com/pages.

LeBaron, B. A., Michalsky, J. J., and Perez, R., 1990: *A simple procedure for correcting shadowband data for all sky conditions.*, Sol Energy, **44**, 249–256.

Li-Cor, 2006: Manual Li-200SA, www.licor.com/env/Products/Sensors/200/li200_description.jsp.

Long, C. N. and Ackerman, T. P., 2000: *Identification of clear skies from broandband pyranometer mesurements and calculation of downwelling shortwave clound effects.*, Journal of Geophysics, **105**, 15 609–15 626.

Long, C. N., Sabburg, J. M., Calbó, J., and Pagès, D., 2006: *Retrieving Cloud Characteristics from Ground-Based Daytime Color All-Sky Images*, J Atmos Ocean Tech, **23**, 633–652.

Michalsky, J. J., Harrison, L., and LeBaron, B. A., 1987: *Empirical radiometric correction of a silicon photodiode rotating shadowband pyranometer.*, Sol Energy, **39**, 87–96.

Michalsky, J. J., Harrison, L. C., and Berkheiser, W. E., 1995: *Cosine response characteristics of some radiometric and photometric sensors.*, Sol Energy, **54**, 397–402.

Ohmura, A., Gilgen, H., Hegner, H., Müller, G., Wild, M., Dutton, E. G., Forgan, B., Fröhlich, C., Philipona, R., Heimo, A., König-Langlo, G., McArthur, B., Pinker, R., Whitlock, C. H., and Dehne, K., 1998: *Baseline Surface Radiation Network (BSRN/WCRP): New Precision Radiometry for Climate Research*, B Am Meteorol Soc, **79**, 2115–2136.

Perez, R., Aguiar, R., Collares-Pereira, M., Dumortier, D., Estrada-Cajigal, V., Gueymard, C., Ineichen, P., Littlefair, P., Lund, H., Michalsky, J., Olseth, J., Renne, D., Rymes, M., Skartveit, A., Vignola, F., and Zelenka, A., 2001: Solar resource assessment: A review. In: Solar Energy - The state of the art. (ISES Position Papers), James & James Science Publishers, London, pp. 497-562.

Raïch, A., 2006: Comparació de les mesures d'irradiància de piranòmetres termoelèctrics i de silici. Efectes de l'altura solar, de la nuvolositat i de la temperatura., Treball de Recerca del Doctorat de Medi Ambient, Universitat de Girona.

Ricchiazzi, P., Yang, S., Gautier, G., and Sowle, D., 1998: *SBDART: A Research and Teaching Software Tool for Plano-Parallel Radiative Transfer in the Earth's Atmosphere.*, B Am Meteorol Soc, **79**, 2101–2114.